

BEAM-BEAM COMPENSATION USING ELECTRON LENS IN RHIC

H. J. Kim, T. Sen, FNAL, Batavia, IL 60510, USA

Abstract

A beam-beam simulation code (BBSIMC) has been developed to study the interaction between counter moving beams in colliders and its compensation through a low energy electron beam. This electron beam is expected to improve intensity lifetime and luminosity of the colliding beams by reducing the betatron tune shift and spread from the head-on collisions. In this paper we discuss the results of beam simulations with the electron lens in the Relativistic Heavy Ion Collider (RHIC). We study the effects of the electron beam profile and strength on the betatron tunes, dynamic aperture, frequency diffusion and beam lifetime.

INTRODUCTION

In high energy storage-ring colliders, the nonlinear effect arising from beam-beam interactions is a major source that leads to the emittance growth, the reduction of beam life time, and limits the collider luminosity. The long-range beam-beam effects can be mitigated by separating the beams to the extent possible. Increasing the luminosity requires higher beam intensity and often focusing the beam to smaller sizes at the interaction points. The effects of head-on interactions become even more significant. The head-on interaction introduces a tune spread due to a difference of tune shifts between small and large amplitude particles. In the proton-proton run of RHIC [1], the maximum beam-beam parameter reached so far is about $\xi = 0.008$. The combination of beam-beam and machine nonlinearities excite betatron resonances which diffuse particles into the tail of beam distribution and even beyond the stability boundary. It is therefore important to mitigate the head-on beam-beam effect.

The compensation of the beam-beam effect with use of low energy electron beam, so called electron lens, has been proposed in particular for a reduction of the large tune spread of proton beam and emittance growth in RHIC [2]. The tune spread is fully compressed by the electron lens with an electron beam profile which matches to a proton beam. Simulation studies showed that the electron lens leads to an increase of beam loss when the electron beam profile matches a proton beam at the lens location and its intensity is chosen to fully compress the tune spread [3]. In this paper, we will discuss the requirements of an electron lens to improve the beam stability and the beam life time.

MODEL

To investigate the effects of an electron lens on tune change and beam loss, a weak-strong tracking code BBSIMC [4] is applied. In the code, the weak beam is rep-

Circular Colliders

A01 - Hadron Colliders

Table 1: RHIC Parameters at Proton-Proton Collision

quantity	unit	Blue ring
beam		proton
energy, γ	Gev/n	107.396
bunch intensity	10^{11}	2
$\epsilon_{x,y}(95\%)$	mm mrad	15
(β_x^*, β_y^*)	m	(0.52, 0.52)
$(\beta_x, \beta_y)^\dagger$	m	(10.4, 9.7)
(ν_x, ν_y)		(28.685, 29.695)
(ξ_x, ξ_y)		(1, 1)
\mathcal{A}_B	eV·s	0.17
$\sigma_{\Delta p/p}$		1.43×10^{-4}
σ_z	m	0.44

\dagger beta function at electron lens location.

resented by macroparticles with the same charge to mass ratio as the beam particles. The transverse and longitudinal motion of particles is calculated by linear transfer maps between nonlinear elements at which nonlinear forces are exerted on the particles. We adopt the weak-strong model to treat the beam-beam interactions. The strong bunch is divided into slices in a longitudinal direction to consider the finite bunch length effect of the beam-beam interaction. In the simulations, we applied 11 slices in the main IPs where the beta function is comparable with the bunch length. Each slice in a beam interacts with particles in the other beam in turn at the collision points. Since the beta function at the electron lens location is much greater than the bunch length, as shown in Table 1, the electron lens is considered as a thin element because the betatron phase advance is negligible over the bunch length.

In order to seek the electron lens parameters at which the beam life time is improved, we choose three different electron beam distribution functions as shown in Fig. 1: (a) $1\sigma_p$ Gaussian distribution with the same rms beam size as that of the proton beam σ_p at the electron lens location (IP10), (b) $2\sigma_p$ Gaussian distribution with rms size twice that of the proton beam, and (c) Smooth-edge-flat-top (SEFT) distribution with an edge around at $4\sigma_p$. The transverse kick on the proton beam from the electron beam is given by

$$\Delta \vec{r}^\dagger = \frac{2\tilde{n}r_0}{\gamma} \frac{\vec{r}_\perp}{r_\perp^2} \zeta(r_\perp : \vec{\sigma}),$$

where \tilde{n} is the number of electrons of the electron beam adjusted by the electron speed, r_0 is the classic proton radius, and γ is the Lorentz factor. The function ζ is given by

- for Gaussian distribution

$$\zeta(r_\perp : \vec{\sigma}) = \left[1 - \exp\left(-\frac{r_\perp^2}{2\vec{\sigma}^2}\right) \right],$$

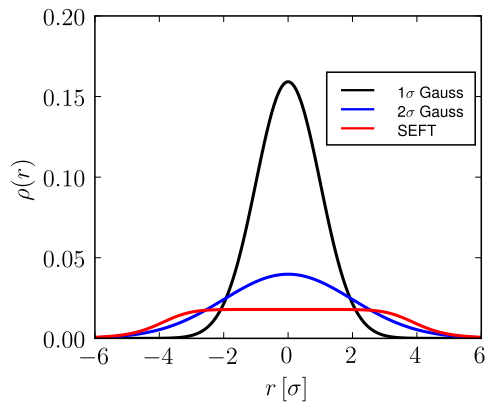


Figure 1: Transverse electron beam distributions: (black) $1\sigma_p$ Gaussian distribution, (blue) $2\sigma_p$ Gaussian distribution, and (red) constant distribution with smooth edge; $\rho(r) \sim \frac{1}{1+(r/4\sigma_p)^8}$.

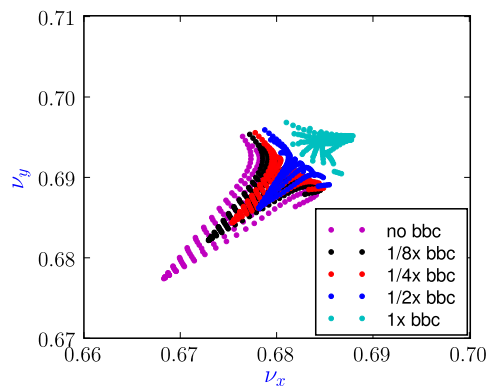


Figure 2: Plot of tune footprints for different electron beam intensities. 1x bbc stands for beam-beam compensation with full electron beam intensity.

- for SEFT distribution

$$\zeta = \frac{\sqrt{2}\tilde{\rho}_0}{8} \left[\frac{1}{2} \log \left(\frac{\theta_+^2 + 1}{\theta_-^2 + 1} \right) + \tan^{-1} \theta_+ + \tan^{-1} \theta_- \right],$$

where $\tilde{\rho}$ is a constant, and $\theta_{\pm} = \sqrt{2} \left(\frac{r}{\sigma} \right)^2 \pm 1$.

SIMULATION RESULTS

In the simulation, we include the nonlinearities such as head-on beam-beam interactions, multipole errors in the interaction region (IR) quadrupole triplets, and sextupoles for chromaticity correction as well as electron lens. Figure 2 shows the tune footprints of on-momentum particles with initial amplitudes in the range 0-6 $\sigma_{x,y}$ for different intensities of $1\sigma_p$ Gaussian electron beam profile. When the electron beam profile matches the proton beam, the full compression of the tune spread requires the electron beam intensity $N_e = N_{ip} \cdot N_p$, where N_{ip} is the number of IPs, and N_p the proton beam intensity. In this study, the electron beam intensity is given by $N_e = 4 \times 10^{11}$ which is defined

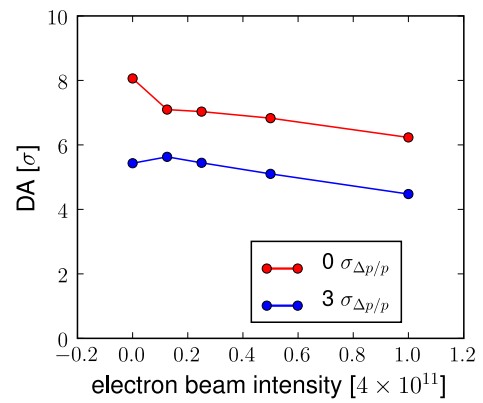


Figure 3: Plot of angle averaged dynamic aperture versus electron beam intensity for on- and off-momentum particles.

as the electron beam intensity required for full compensation or 1x bbc. As shown in Fig. 2, the 1x bbc shrinks the tune spread to about 30% of the spread without an electron lens while footprint folding is observed at small amplitude. The small electron intensity compresses the tune spread partially without inducing further the footprint folding.

Figure 3 shows angle-averaged dynamic apertures of on- and off-momentum particles for different intensities of the $1\sigma_p$ Gaussian electron beam profile. The dynamic aperture is calculated as the largest radial amplitude of particle that survives after 10^6 turn tracking at different phase angles. The dynamic apertures of on-momentum particles decreases as the electron intensity increases. However, the dynamic aperture of off-momentum particles has a peak at $\frac{1}{8}$ x bbc and does not decrease up to $\frac{1}{4}$ x bbc. Even a small increment in the dynamic aperture may help to reduce a beam loss because there is a high chance of loss for off-momentum particles.

Frequency diffusion maps are found by calculating a variation of the betatron tunes over two successive sets of N turns, where N is typically some appropriate power of two. These maps are shown in Fig. 4 to investigate the effect of electron lens compensation. A large tune variation is generally an indicator of reduced stability. Both 1x bbc and $\frac{1}{2}$ x bbc increase the detuning of betatron tunes and make the particle motions more chaotic at amplitude beyond 3σ while the detuning is suppressed at small amplitude. However, the diffusion map of $\frac{1}{8}$ x bbc shows more stable motion over a larger range of amplitudes compared to motion without an electron lens.

Figure 5 shows the results of particle loss in 1×10^6 turns for different intensities with the $1\sigma_p$ Gaussian electron beam profile. At an intensity of 1x bbc, the particle loss is nearly six times the loss without beam-beam compensation. The beam lifetime of $\frac{1}{2}$ x bbc however is comparable with that of no bbc. As the electron beam intensity is decreased, the particle loss decreases significantly below $\frac{1}{4}$ x bbc, and is reduced to 30% of no bbc at $\frac{1}{8}$ x

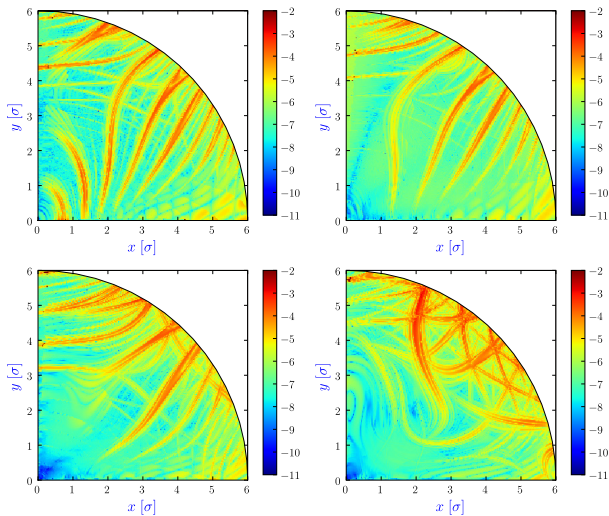


Figure 4: Plot of frequency diffusion map of betatron tunes: (top left) no electron lens, (top right) $\frac{1}{8}x$ bbc, (bottom left) $\frac{1}{2}x$ bbc, and (bottom right) $1x$ bbc. The tune change is logarithmically scaled by $\log \sqrt{\Delta\nu_x^2 + \Delta\nu_y^2}$.

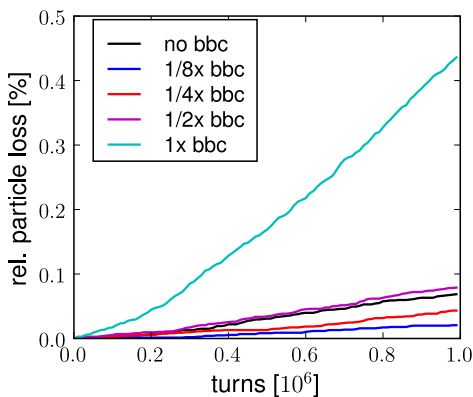


Figure 5: Plot of particle loss according to electron beam intensity for a $1\sigma_p$ Gaussian electron beam profile.

bbc. This is somewhat correlated to the dynamic aperture since the stability boundary is slightly larger at $\frac{1}{8}x$ bbc, as shown Fig. 3 and 4.

For the $2\sigma_p$ Gaussian and SEFT electron beam profiles, we calculated dynamic apertures, frequency diffusion maps and particle loss for different electron beam intensities. The results are summarized in Table 2.

The upper limits of the electron beam intensity for the two distributions are chosen so that peak of the electron profile is matched to that of $1x$ bbc at $1\sigma_p$ Gaussian. For the $\frac{1}{2}x$ bbc and $1x$ bbc of $2\sigma_p$ Gaussian profile, there is a small increase in the dynamic aperture of off-momentum particles. There is however a significant reduction in beam loss, for example, below 10% of the particle loss without beam-beam compensation when the electron beam intensity is $\frac{1}{2}x$ bbc. The dynamic aperture obtained with the SEFT profile remains almost the same up to $2x$ bbc. Nevertheless a significant improvement of beam lifetime is also observed below $2x$ bbc. There is a threshold electron

Table 2: Comparison of Dynamic Apertures and Particle Loss for Different Electron Beam Profiles and Intensities

Profile	Intensity ($N_{ip} \cdot N_p$)	DA (σ)	Particle loss [†] (%)
$1\sigma_p$ Gaussian	1	4.48	635
	1/2	5.10	115
	1/4	5.44	63
	1/8	5.63	30
$2\sigma_p$ Gaussian	4	3.53	93
	2	5.05	10
	1	5.40	8
	1/2	5.63	6
SEFT	8	3.60	330
	4	4.77	21
	2	5.46	22
	1	5.47	6
	1/2	5.57	6

[†]relative to that without beam-beam compensation

beam intensity below which beam life time is increased: $\frac{1}{2}x$ bbc for the $1\sigma_p$ Gaussian, $2x$ bbc for the $2\sigma_p$ Gaussian, and $4x$ bbc for the SEFT profile. Particle loss is relatively insensitive to electron lens current variations below threshold current with the $2\sigma_p$ Gaussian and SEFT profiles. This looser tolerance on the allowed variations in electron intensity is likely to be beneficial during experiments.

SUMMARY

In this paper, we investigated the effects of different electron lens profiles and intensities on proton beam lifetime. Full tune-spread compression causes footprint folding and increases particle loss while partial tune-spread compression does not induce footprint folding and may reduce particle loss. We observe a closer correlation between particle loss and frequency diffusion than with the dynamic aperture. There is a threshold electron beam intensity below which proton beam life time is increased. Particle losses for the $2\sigma_p$ Gaussian and SEFT profiles are relatively insensitive to intensities below threshold. A wider electron beam profile than the proton beam at the electron lens location is found to increase beam life time.

ACKNOWLEDGMENTS

We thank Y. Luo for help with the RHIC lattice. This work was supported by the US-LARP collaboration which is funded by the US Department of Energy.

REFERENCES

- [1] C. Montag et al., Proceedings of EPAC08, p2566 (2008).
- [2] Y. Luo and W. Fischer, BNL-CAD/AP/286 (2007).
- [3] A. Valishev et al., LARP Mini-Workshop on Electron Lens Simulations at BNL (2008).
- [4] H.J. Kim et al., PRST-AB **12**, 031001 (2009).